

QUANTIFYING NOISE INDUCED EFFECTS
IN THE GENERIC DOUBLE-WELL POTENTIAL*B. DYBIEC[†], E. GUDOWSKA-NOWAK[‡]Marian Smoluchowski Institute of Physics
and Mark Kac Center for Complex Systems Research, Jagellonian University
Reymonta 4, 30-059 Kraków, Poland*(Received April 27, 2007)*

Contrary to conventional wisdom, the transmission and detection of signals, efficiency of kinetics in the presence of fluctuating barriers or system's synchronization to the applied driving may be enhanced by random noise. We have numerically analyzed effects of the addition of external noise to a dynamical system representing a bistable over-damped oscillator and detected constructive influence of noise in the phenomena of resonant activation (RA), stochastic resonance (SR), dynamical hysteresis and noise-induced stability (NES). We have documented that all above-mentioned effects can be observed in the very same system, although for slightly different regimes of parameters characterizing external periodic driving or (and) noise. Particular emphasis has been given to presentation of various quantifiers of the noise-induced constructive phenomena and their sensitivity to the location and character of the imposed boundary condition.

PACS numbers: 05.40.-a, 05.10.-a, 02.50.-r, 82.20.-w

1. Introduction

The formulation of the fluctuation theory by Einstein and by Smoluchowski has opened a new road towards understanding statistical physics within the framework of stochastic processes. In particular, the quantitative explanation of the Brownian motion as a realization of random walk and mathematical development of the theory presented in the pioneering works by Langevin and Wiener have created foundations for the dynamical interpretation of motion under the influence of irregular, noisy forces, provoking

* Presented at the XIX Marian Smoluchowski Symposium on Statistical Physics, Kraków, Poland, May 14-17, 2006.

[†] bartek@th.if.uj.edu.pl

[‡] gudowska@th.if.uj.edu.pl

an outburst of studies on fluctuation-facilitated transport and fluctuation-induced critical phenomena. In nonlinear systems, a combined action of external driving and noise has been demonstrated [1–4] to induce the whole plethora of unexpected effects whose appearance and action can be understood by proper interpretation of non-equilibrium, dissipative dynamics.

In this paper, the generic double-well, periodically modulated potential model perturbed by thermal Gaussian fluctuations is investigated. By use of the numerical Monte Carlo methods all known effects displaying constructive role of noises are demonstrated. In order to predict diverse physical manifestations of the cooperative behaviors between the noise and input periodic “signal”, various quantifiers of noise-induced effects are examined and detection of stochastic resonance (SR), resonant activation (RA), dynamical hysteresis and noise enhanced stability (NES) is evidenced in the same dynamical system, although for different regimes of feature parameters.

Our analysis starts with the phenomenon of stochastic resonance [1, 3] which predicts optimization and synchronization of the system’s response in the presence of noise. Occurrence of the phenomenon was experimentally proven in digital devices such as Schmitt triggers [2] and observed in physical systems such as ring lasers [5], vertical cavity surface emitting lasers [6] or colloidal suspensions [7]. Characteristic features of SR were also recognized in biological systems [4, 8–11]. In SR, due to interaction between the input signal and the system, weak input signal can be amplified by its stochastic counterpart. An increase of the noise intensity to a certain optimal level improves the output signal quality as measured by signal-to-noise ratio (SNR), spectral power amplification (SPA) or residence time distribution [12, 13].

Another phenomenon manifesting constructive role of noises is the resonant activation which describes the most efficient time-averaged escape rate over a time-modulated energy barrier. The cooperative interplay between time-dependent modulation of the barrier and thermal fluctuations that assist the motion over the barrier cause the enhancement of the kinetic rate for the process. In consequence, the RA is a generic effect for barrier crossing events in conformation-modulated energy landscape [4, 14].

Owing to the different nature of SR and RA, the system’s response to a periodic signal generally cannot be optimized simultaneously for both phenomena to occur. Comparative experimental studies with a colloidal particle trapped in the double-well potential created by optical tweezers [7, 15] have shed a light on differences between the two effects.

Bistable systems reacting to the external periodic stimulus may also exhibit a time-delayed “hysteretical” response to the cyclical variation of a control parameter [16, 17]. In particular, it has been argued that the hysteresis loop area can be a useful quantity for identifying critical values of field parameters responsible for the onset of resonance-like response of the

system and therefore helpful in designing field parameters for an optimal control [16–18]. In fact, the maximal loop area of the dynamical hysteresis is indicative of the highest level of synchronization between the state of the process and the external stimulus and can be correlated with occurrence of the SR.

In resonant activation, dynamical hysteresis and stochastic resonance presence of noise positively influences kinetics and makes it more efficient and synchronized. On the contrary, the optimal level of noise can also prolong the amount of time that the process spends in a metastable state, thus modifying the stability of the system and inhibiting the process of passage over the barrier. The effect known as the noise enhanced stability (NES) [19] is also closely related to the noise-induced stabilization and noise-induced slowing down [20].

Usually phenomena manifesting constructive role of noises in physical systems have been considered separately. Here it is shown that all known noise-induced phenomena (resonant activation, stochastic resonance, synchronization, dynamical hysteresis and noise enhanced stability) could be observed in the same system. Depending on the quantities under the study and their interpretation, various effects could be recorded. The coexistence of these effects suggests that they are very closely related and should be considered together.

2. Model

For the examination of the noise induced effects in the generic double-well potential the Langevin equation

$$\frac{dx(t)}{dt} = -V'(x) - \underbrace{A_0 \cos(\Omega t + \varphi)}_{f(t)} + \xi(t), \quad (1)$$

describing motion of the over-damped Brownian particle has been used. Here $V(x)$ represents the static double-well potential of the fourth order

$$V(x) = -\frac{a}{2}x^2 + \frac{b}{4}x^4. \quad (2)$$

whose minima are located at $x_m = \pm\sqrt{a/b}$ with a separating maximum located at $x_b = 0$. The depth of the unperturbed potential well is equal to $V(x_b) - V(x_m) = \Delta V = a^2/(4b)$. For the purpose of simulations $a = 128$, $b = 512$ and $A_0 = 8$, *i.e.* $x_m = \pm\frac{1}{2}$ and $\Delta V = 8$. $\xi(t)$ is a delta correlated, $\langle \xi(t)\xi(t') \rangle = \sigma^2\delta(t - t')$, white noise of intensity σ^2 . A particle mass, a friction coefficient and the Boltzmann constant has been preset to 1.

The periodic forcing $f(t)$ causes the periodic modulation of the potential

$$V(x) + A_0 x \cos(\Omega t + \varphi) = V(x) + A_0 x \cos \left[\frac{2\pi}{T_\Omega} t + \varphi \right].$$

As the consequence, the crossings over the barrier as described by the transition probabilities of the thermally activated hops become time dependent. For Brownian particle performing motion within the periodically tilted potential a maximum synchronization between the thermally activated hopping and the weak periodic driving occurs when the Kramers time matches time scale of the modulation T_Ω . During the motion, the local stability of the potential minima changes, *i.e.* part of the driving force's period the left potential minimum can be favored over the right, while during the remaining part of time the right minimum is more stable. Moreover, the periodic driving $f(t)$ shifts the positions of x_m (potential minima) and x_b (separation surface), as indicated in Fig. 1.

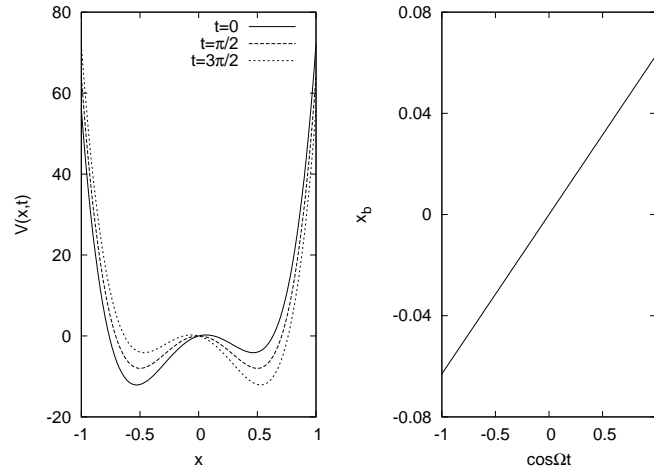


Fig. 1. Modulation of the generic double-well potential (left panel) $-ax^2/2+bx^4/4+A_0x\cos\Omega t$ with $a = 128$, $b = 512$, $A_0 = 8$, $\Omega = 1$ for $t = \{0, \pi/2, 3\pi/2\}$ and the location of the top of the potential barrier (right panel) as a function of $\cos\Omega t$. The preferable direction of the motion in the presence of a non-biased noise is from a shallower to a deeper minimum. For a chosen set of parameters potential maxima are always separated by a local maximum of the potential.

The Langevin equation Eq. (1) was integrated by standard techniques of integration of stochastic differential equations with respect to the Wiener process [21]. Properties of the system were examined by use of the Monte Carlo techniques. Long realizations of the non-stationary process governed by Eq. (1) were simulated and collected ensembles of trajectories were used to estimate various quantifiers of noise-induced effects.

3. Solutions and results

The interplay of external driving and thermal fluctuations leads to several above-mentioned fine-tuning properties of the system. All those phenomena can be registered in the analysis of the generic model and the conditions for their occurrence are clarified. Finally, the related effect of noise enhanced stability, which is also observed in a subject to noise, modulated double-well potential, is discussed.

3.1. Stochastic resonance

As already stated, the stochastic resonance phenomenon typically occurs in nonlinear systems when the stochastic noise amplifies a weak periodic input signal [1]. An explanation of the phenomenon may be given in terms of different characteristics. Measures of the stochastic resonance could be based on the measurement of the input-output synchronization (periodic response, spectral amplification, area of the dynamical hysteresis loop, residence time distribution) or extraction of the signal from the background noise (signal-to-noise ratio).

In Fig. 2 sample power spectrum of the process governed by Eq. (1) is presented. From power spectra, spectral amplification $\eta(\sigma^2)$ and signal-to-noise ratio (SNR), according to definition from [1], were estimated. In the power spectrum clear peak at the driving frequency $\omega \approx \Omega = 1$ is visible.

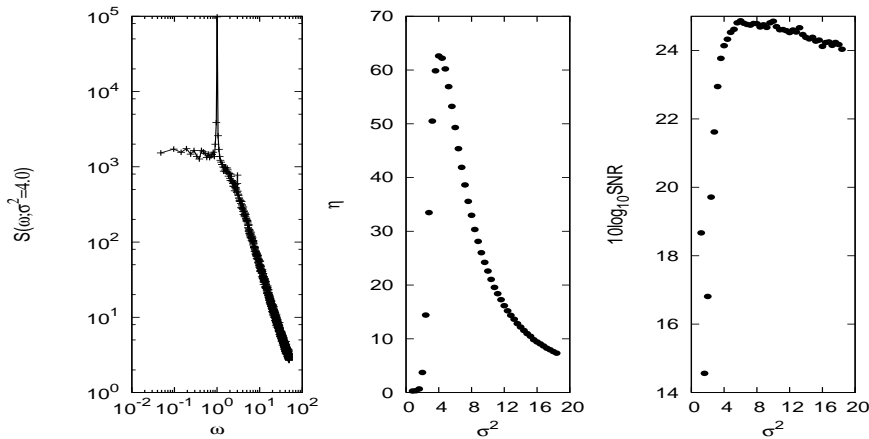


Fig. 2. The power spectrum $S(\omega)$ for $\sigma^2 = 4$, the spectral amplification $\eta(\sigma^2)$ and SNR for the generic model. The maximum of SNR corresponds to the situation when the signal is extracted from the background noise in the optimal way. The maximum of the spectral amplification η represents such a value of the noise intensity that the system reproduces the input signal in the best way. The frequency of external driving $\Omega = 1$.

Inspection of the spectral amplification and signal-to-noise ratio indicates the existence of an optimal noise intensity σ^2 for which the quantifiers of stochastic resonance are maximal.

Motion of the heavily damped Brownian particle in a tilted double-well potential is registered in stochastic trajectories $x(t)$ exhibiting a series of switchings between both sides of the potential barrier. In the absence of the periodic forcing, the residence time distribution (*i.e.* distribution of time episodes in which the process $x(t)$ dwells in a right/left potential well) is exponential. An introduction of the periodic driving produces series of peaks centered at $T_n = (n + \frac{1}{2})T_\Omega$ with $n = 0, 1, 2, \dots$. These peaks are centered at preferable times for the most probable particle passage when the relevant potential barrier height becomes minimal. After a transition, the particle has to wait for the half of the period $T_\Omega/2$ before the next best chance for the reverse passage happens.

An analysis of histograms of residence times when the system dwells on one of the meta-stable states provides another measure of the stochastic resonance [12, 13]. The presence of peaks indicates the level of the synchronization between the switching mechanism and the external periodic driving. Barrier crossing events tend to take place when the external driving assists the noise in moving a particle from one potential well to another, *i.e.* when the relative barrier is minimal. In particular, the area under the first peak, *cf.* right panel of Fig. 4, which is located at $T_\Omega/2$, is the measure of the synchronization between the input and the output signals. It becomes the largest in the regime SR, when the switchings between the potential wells are in phase with the external periodic signal and the mean residence time is closest to half the signal period. Fig. 3 presents sample residence time distributions for various values of the noise intensity σ^2 . The right panel of Fig. 4 presents numerical estimation of the area under the first peak of the residence time distributions.

For large t ($t \rightarrow \infty$), the process $x(t)$ described by Eq. (1) loses information about its initial state and the average $\langle x(t) | x(0) = x_0 \rangle$ becomes a periodic function of time with dominant frequency equal to the frequency of external driving $\Omega = 1$ [1, 3], *i.e.* $\langle x(t) \rangle_{\text{as}} = \bar{x} \cos(\Omega t - \bar{\varphi})$ where the amplitude \bar{x} and the phase shift $\bar{\varphi}$ depend on the noise intensity σ^2 and the frequency of the external driving Ω . In left panel of Fig. 4 the amplitude of $\langle x(t) \rangle_{\text{as}}$ *versus* the noise intensity σ^2 is plotted. There exists such a value of σ^2 for which \bar{x} is maximal. Accordingly, at this point the phenomenon of the stochastic resonance takes place.

Evaluation of the area, P_1 , under the first peak of the residence time distribution, due to presence of the exponential background produced by spontaneous transitions between states, is complicated and not fully unique. Usually, this problem is resolved by subtracting exponential decay or by restricting the area of integration to a smaller arbitral interval than $[0, T_\Omega]$.

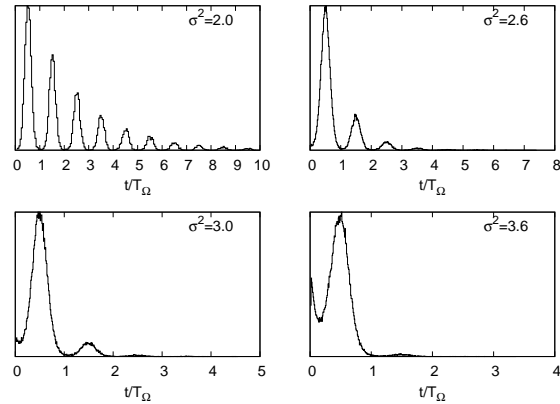


Fig. 3. Residence time distributions for the generic model for various noise intensities. For a large noise intensity, the particle moving in a double-well potential does not feel the potential barrier and the residence time distribution approaches the exponential distribution. For small noise intensities, the barrier crossing events are most efficient when the potential barrier attains its minimum. Therefore, the residence time distribution consists of periodic peaks centered at time points when the height of the surface separating the minima of the potential is minimal.

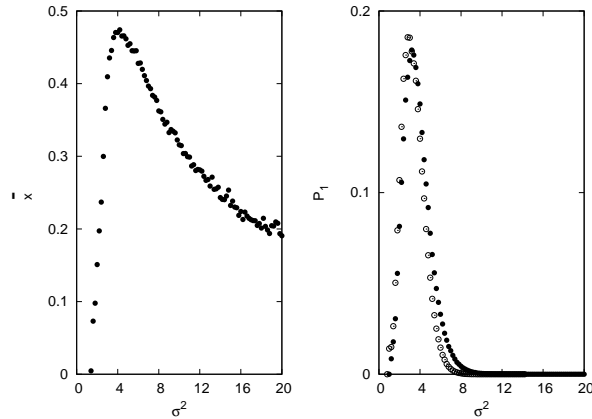


Fig. 4. The amplitude \bar{x} of $\langle x(t) \rangle_{as}$ (left panel). The maximum of $\bar{x}(\sigma^2)$ corresponds to the noise intensity for which the cleanest output signal is visible. The area P_1 under the first peak of the residence time distribution (right panel). The maximum of $P_1(\sigma^2)$ corresponds to the noise intensity for which the best synchronization of the stochastic process with the external periodic driving takes place. Empty dots: the border between states is located at the top of the perturbed potential, full dots: the border between states is located at the minimum of the unperturbed potential.

Therefore, to avoid this problems, as a measure of the stochastic resonance probability, $P(\dots, T_\Omega)$, of a given number of transitions between states during one period of the external driving, T_Ω , has been suggested [22]. Samples of $P(\dots, T_\Omega)$ probabilities are presented in Fig. 5.

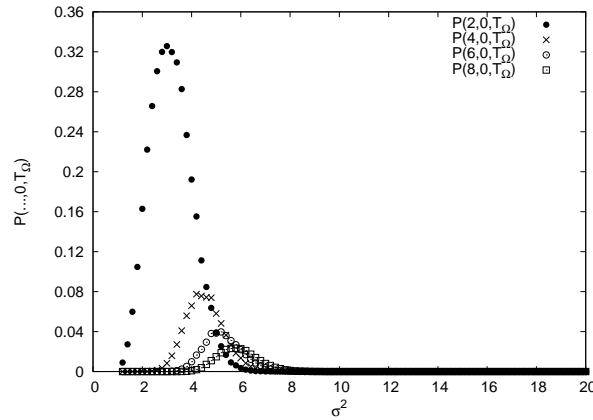


Fig. 5. Probability, $P(\dots, T_\Omega)$, of given number of transitions between states during one period, T_Ω , of the external driving. For clarity of the plot only probabilities of exactly 2, 4, 6, 8 transitions in the time interval $[0, T_\Omega)$ are depicted.

3.2. Resonant activation

First passage time problem for a given stochastic process concentrates on calculation of the time-dependent probability density for a process $\{x(t)\}$ to reach for the first time a point x or to cross a boundary. In this section we discuss evaluation of the mean value of the first passage time (MFPT) distribution (see Fig. 6) when crossing a boundary may be understood as

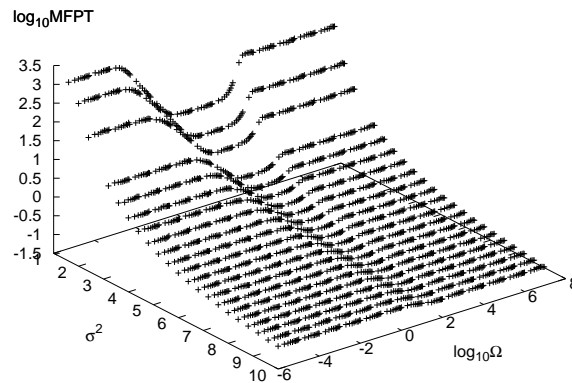


Fig. 6. MFPTs' surface.

an escape event from one of the potential wells [23]. Accordingly, MFPT is then defined as an average time after which the particle becomes absorbed (removed from the system). Figs. 6, 7 present results of MFPT *versus* the angular frequency of the external driving Ω for various noise intensities σ^2 . In the simulations, the particle starts its diffusive motion in the left potential minimum. The absorbing boundary is located at the maximum of the perturbed potential. Histograms of FPTs were estimated from the trajectories $x(t)$ and consequently the MFPTs were evaluated.

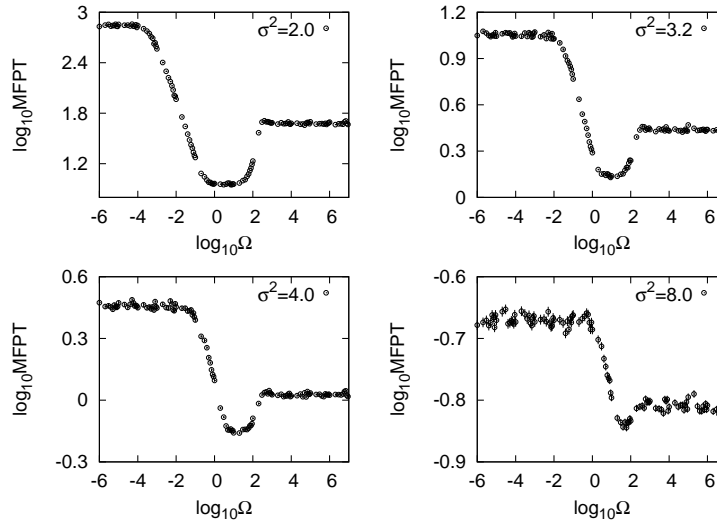


Fig. 7. MFPTs' curves for the periodically modulated double-well potential model with various noise intensities. With an increasing noise intensity the average time that a particle needs to escape from the system decreases.

As it can be seen in Fig. 7, the dependence of MFPT on the driving angular frequency Ω is non monotonic [24] and for certain value of the external driving frequency Ω_{res} the MFPT becomes minimal. The observed RA phenomenon [14] corresponds to the maximal reaction rate [23] and decreases with the increasing noise intensity σ^2 when the separatrix surface between the wells is no longer experienced by the moving particle.

Although RA and SR phenomena seem to be interrelated [14, 25, 26], the conditions for both effects to be observed are different. The RA response is observed at a fixed value of the noise intensity σ^2 after tuning the driving frequency Ω to a resonant value Ω_{res} whereas SR is typically examined as a function of the noise intensity. Nevertheless, both effects are visible in the same parameter regime.

3.3. Dynamical hysteresis loop

Fig. 8 presents the probability of finding a particle in the right potential well as the function of the external driving. Due to periodic perturbation of the potential barrier, the probability density function of the variable $x(t)$ becomes periodic and, as a consequence, the probability of finding a process in one of the potential wells is a looping function of time. In the simulations, the separating surface between potential wells is located at the maximum of the perturbed potential, Fig. 1. The area of the dynamical hysteresis loop changes with the noise intensity [18] and can be optimized for detecting its maximum *cf.* Fig. 9. Interestingly, the noise intensity for which the spectral amplification $\eta(\sigma^2)$ (and $\bar{x}(\sigma^2)$) attains maximum is slightly different from the value of the noise intensity for which the area of the dynamical hysteresis loop is maximal. It is due to the fact that the spectral amplification as well as the amplitude of the periodic response take into account different characteristics of the process $x(t)$ [17, 18].

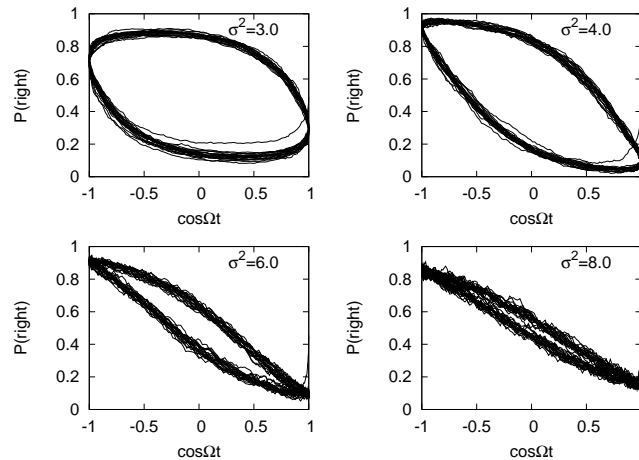


Fig. 8. Dynamical hysteresis loops for various noise intensities. With the increasing value of the noise intensity the area of the dynamical hysteresis loop decreases. It is the effect of the fact that the increasing noise intensity decreases the phase shift between the periodic input signal and the periodic response of the system.

In Table I, summary of our evaluations is displayed. The most popular performance measures of SR are presented pointing to the sensitive role played by properly posed boundary conditions. More precisely, we observe that due to possible recrossings, evaluation of maximal P_1 is recorded for different noise intensities when the barrier dividing the states is placed at the other minimum of the unperturbed potential, or at the perturbed potential top. Moreover, evaluation of hysteresis loop area indicates that its maximum

TABLE I

Values of the noise intensity for which maxima of SR measures are recorded. Location of the maximum of SNR, due to flat character of SNR curve, is not included.

Measure	Border location	σ^2
periodic response (\bar{x})	none	4.2
spectral amplification (η)	none	4.0
$P(2, 0, T_\Omega)$	minimum of the unperturbed potential	3.0
P_1	barrier top of the perturbed potential	2.8
P_1	minimum of the unperturbed potential	3.2
hysteresis loop area	barrier top of the perturbed potential	3.2

is observed for the same noise intensity σ^2 for which largest P_1 is recorded for trajectories reaching the other minimum of the unperturbed potential.

A double-well potential with an additive periodic driving tuning the relative stability of states is an archetypal model used in a variety of biological applications. The similar model, based on a special form of the double-well potential was used for description of a voltage-gated ion channel in a red blood cell [27] in which a dynamical hysteresis was observed experimentally.

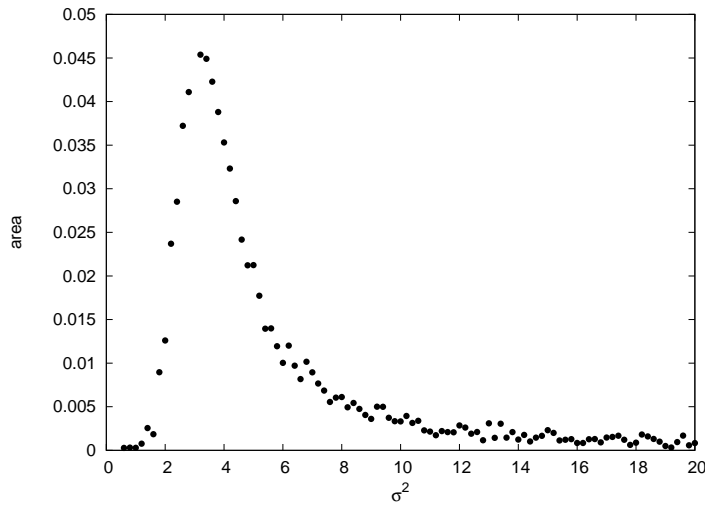


Fig. 9. Area of the hysteresis loop.

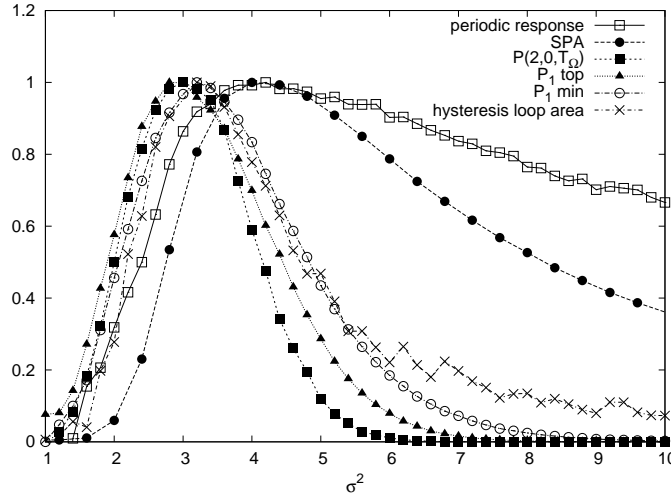


Fig. 10. Considered measures of SR. For better comparisons, measures are normalized in such a way that a maximal value of each measure is equal to one.

3.4. Noise enhanced stability

Finite amount of noise intensity may also enhance the lifetime of an unstable state. The phenomenon, addressed in physical literature as noise enhanced stability (NES) was observed both, in linear [19] and cubic potentials [20]. By investigating the escape times from a time modulated metastable state, the same effect can be detected in the generic double-well potential model. Left panel of Fig. 11 displays the perturbed generic double-well potential at various times t . The particle starts its motion at the $x_0 = 0.22$ and continues until the absorption at $x_b = 0.5$ takes place. Results of numerical evaluation of corresponding mean first passage times MFPTs for the problem are shown in the right panel of Fig. 11. The solid line indicates an analytical result [23] for passages over the static barrier, *i.e.* with $\varphi = \pi$ and $\Omega = 0$ (*cf.* Eq. (1)). The dashed lines stand for the deterministic evaluation of the MFPTs over the static, *i.e.* $A_0 = 0$, (lower dashed line) and modulated (upper dashed line) potential barrier. In Monte Carlo simulations this limit is reached for noise intensities σ^2 tending to zero. Addition of weak noise causes MFPT to increase steadily up to the maximal value from which further decrease of the MFPT is observed. For static and modulated potentials a clear feature of the NES phenomenon is observed: there exists a critical value of the noise intensity σ^2 for which the MFPT attains the maximum. In general, by choosing an appropriate potential, boundary and initial conditions the lifetime of a metastable state can be arbitrarily prolonged [20].

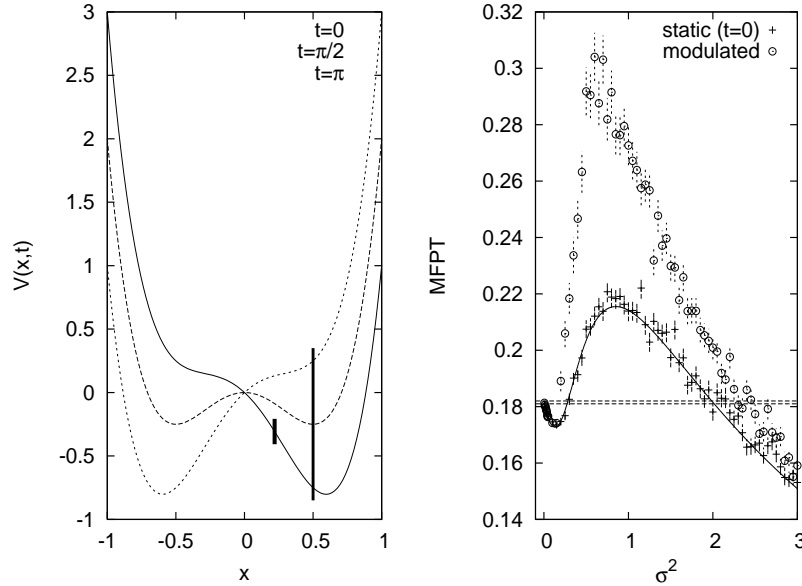


Fig. 11. The generic perturbed double-well potential (1) (left panel) with $a = 4$, $b = 16$, $A_0 = 1$, $\Omega = 1$, $\varphi = \pi$. Bold lines represent the starting point and the absorbing boundary. Particle starts its motion at $x_0 = 0.22$ and continues until absorption at $x_b = 0.5$. In the right panel, the solid line stands for MFPTs for the static potential, *i.e.* the potential of the form of the perturbed potential at time $t = 0$. Points represent Monte Carlo simulations for the static and periodically modulated potential barrier with $\Omega = 1$. Others parameter are $N = 10^4$, $\Delta t = 10^{-5}$. Dashed lines represent deterministic MFPTs over the static (lower dashed line) and modulated potential barrier (upper dashed line), details in the text. Error bars represent deviation of the mean.

4. Summary and conclusions

The double-well potential model provides an excellent setup to examine resonant effects induced by combined action of noises and periodic forcing. Our studies confirm possibility of detection of the SR, RA, NES and dynamic hysteresis phenomena in the over-damped Brownian dynamics taking place in a periodically modulated double-well potential model. Table I, central to the discussion of the results presented here clearly demonstrates that (i) maximal values of the same SR measure will be observed for different noise intensities if various border locations between the states are specified, (ii) in general, characterization of SR is non-unique and the definition of the phenomenon will depend in many respects on a chosen feature quantity as calculated or measured in the system. Given the fact that all of diverse

“noise-induced” phenomena can be observed for signals described by the same standard model, one can muse about possible concerted realizations of such optimized actions in natural systems whose performance depends on modulation frequency and intensity of thermal noise.

The Authors acknowledge the financial support through the Marie Curie TOK COCOS grant (6th EU Framework Programme under contract: MTKD-CT-2004-517186) and the ESF funds via the STOCHDYN program. Additionally, B.D. acknowledges the support from the Foundation for Polish Science and the hospitality of the Humboldt University of Berlin and the Niels Bohr Institute (Copenhagen). Computer simulations have been performed at the Academic Computer Center CYFRONET AGH, Kraków.

REFERENCES

- [1] L. Gammaitoni, P. Hänggi, P. Jung, F. Marchesoni, *Rev. Mod. Phys.* **70**, 223 (1998).
- [2] V.S. Anishchenko, A.B. Neiman, in *Stochastic Dynamics*, Eds. L. Schimansky-Geier, T. Pöshel, Springer Verlag, Berlin 1997, p. 155.
- [3] V.S. Anishchenko, A.B. Neiman, F. Moss, L. Schimansky-Geier, *Phys. Usp.* **42**, 7 (1992).
- [4] R.D. Astumian, F. Moss, *Chaos* **8**, 533 (1998).
- [5] B. McNamara, K. Wiesenfeld, R. Roy, *Phys. Rev. Lett.* **60**, 2626 (1988).
- [6] G. Giacomelli, F. Marin, I. Rabbiosi, *Phys. Rev. Lett.* **82**, 675 (1999).
- [7] D. Babič, C. Schmitt, I. Poberaj, C. Bechinger, *Europhys. Lett.* **67**, 158 (2004).
- [8] S.M. Bezrukov, I. Vodyanoy, *Nature* **385**, 319 (1997).
- [9] A. Fuliński, *Phys. Rev.* **E52**, 4523 (1995).
- [10] P. Hänggi, *Chem. Phys. Chem.* **3**, 285 (2002).
- [11] P. Hänggi, G. Schmid, I. Goychuk, *Nova Acta Leopoldina* **88**, 17 (2003).
- [12] L. Gammaitoni, F. Marchesoni, S. Santucci, *Phys. Rev. Lett.* **74**, 1052 (1995).
- [13] F. Marchesoni, L. Gammaitoni, F. Apostolico, S. Santucci, *Phys. Rev.* **E62**, 146 (2000).
- [14] Ch.R. Doering, J.C. Gadoua, *Phys. Rev. Lett.* **69**, 2318 (1992).
- [15] C. Schmitt, B. Dybiec, P. Hänggi, C. Bechinger, *Europhys. Lett.* **74**, 937 (2006).
- [16] P. Jung, G. Gray, R. Roy, P. Mandel, *Phys. Rev. Lett.* **65**, 1873 (1990).
- [17] M.C. Mahato, A.M. Jayannavar, *Physica A* **248**, 138 (1998).
- [18] J. Juraszek, B. Dybiec, E. Gudowska-Nowak, *Fluct. Noise Lett.* **5**, L259 (2005).
- [19] N.V. Agudov, B. Spagnolo, *Phys. Rev.* **E64**, 035102 (2001).
- [20] A. Fiasconaro, D. Valenti, B. Spagnolo, *Physica A* **325**, 136 (2003).

- [21] D.J. Higham, *SIAM Rev.* **43**, 525 (2001).
- [22] P. Talkner, L. Machura, M. Schindler, P. Hänggi, J. Łuczka, *New J. Phys.* **7**, 14 (2005).
- [23] P. Hänggi, P. Talkner, M. Borkovec, *Rev. Mod. Phys.* **62**, 251 (1990).
- [24] A.L. Pankratov, M. Salerno, *Phys. Lett.* **A273**, 162 (2000).
- [25] B. Dybiec, E. Gudowska-Nowak, *Phys. Rev.* **E66**, 026123 (2002).
- [26] B. Dybiec, E. Gudowska-Nowak, P.F. Góra, *Int. J. Mod. Phys.* **C13**, 1211 (2002).
- [27] E. Gudowska-Nowak, B. Dybiec, H. Flyvbjerg, *Proc. SPIE* **5467**, 223 (2004).